

## Supplementary Information

### Amorphous Nanoparticles by Self-assembly: Processing for Controlled Release of Hydrophobic Molecules

Jie Feng<sup>1,2</sup>, Yingyue Zhang<sup>2</sup>, Simon A. McManus<sup>2</sup>, Rolane Qian<sup>3</sup>, Kurt D. Ristroph<sup>2</sup>, Hanu Ramachandruni<sup>4</sup>, Kai Gong<sup>5,6</sup>, Claire E. White<sup>5,6</sup>, Aditya Rawal<sup>7</sup>, Robert K. Prud'homme<sup>2\*</sup>

*1. Department of Mechanical Science and Engineering, University of Illinois at Urbana-Champaign, Urbana, Illinois 61801, United States*

*2. Department of Chemical and Biological Engineering, Princeton University, Princeton, New Jersey 08544, United States*

*3. Department of Chemical and Biomolecular Engineering, University of Maryland, College Park, Maryland 20742, United States*

*4. Medicines for Malaria Venture, Route de Pré-Bois 20, 1215 Meyrin, Switzerland*

*5. Department of Civil and Environmental Engineering, Princeton University, Princeton, New Jersey 08544, United States*

*6. Andlinger Center for Energy and the Environment, Princeton University, Princeton, New Jersey 08544, United States*

*7. Nuclear Magnetic Resonance Facility, Mark Wainwright Analytical Centre, University of New South Wales, Sydney, Australia*

#### Information of AFFINSOL™ HPMCAS

Table S1. Specification of AFFINSOL™ HPMCAS (<https://www.dow.com/en-us/pharma/products/affinisol>)

\*Corresponding author: prudhomm@princeton.edu

AFFINISOL™ HPMCAS			
	716	912	126
Hydroxypropyl	5.0-9.0%	5.0-9.0%	6.0-10.0%
Methoxyl	20.0-24.0%	21.0-25.0%	22.0-26.0%
Viscosity*	2.4-3.6 cP	2.4-3.6 cP	2.4-3.6 cP
Residue on Ignition	<0.20%	<0.20%	<0.20%
Loss on Drying	<5.0%	<5.0%	<5.0%
Free Acids	<1.0%	<1.0%	<1.0%
Acetate Substitution	5.0-9.0%	7.0-11.0%	10.0-14.0%
Succinate Substitution	14.0-18.0%	10.0-14.0%	4.0-8.0%
Acetic Acid	0.5%	0.5%	0.5%

### Calculation of effective Reynolds number for MIVM

The definition of effective Reynolds number is

$$Re = \sum_{i=1}^4 \frac{U_i D_i}{\nu_i}, \quad (1)$$

where  $U_i$  is the velocity,  $\nu_i$  is the kinematic viscosity of stream  $i$ , and  $D_i$  is the characteristic dimension [1]. The current MIVM set-up has a cross-section area of each inlet as  $1.1 \times 1.5 \text{ mm}^2$  and the diameter of the mixing geometry as  $D_i = 6 \text{ mm}$ . Tables S2, S3 and S4 list the flow velocities and kinematic viscosities of each stream for HPMCAS, zein and lecithin NPs. Therefore, the effective Reynolds numbers are  $Re = 1.2 \times 10^4$ ,  $0.87 \times 10^4$  and  $0.70 \times 10^4$  for HPMCAS, lecithin and zein NPs, respectively.

Table S2. Velocity and kinematic viscosity of each stream for the formulation of HPMCAS NPs

	Organic stream 1	Aqueous stream 2	Aqueous stream 3	Aqueous stream 4
$U_i$ (m/s)	0.16	0.48	0.48	0.48
$\nu_i$ (m <sup>2</sup> /s)	$0.54 \times 10^{-6}$	$0.89 \times 10^{-6}$	$0.89 \times 10^{-6}$	$0.89 \times 10^{-6}$

Table S3. Velocity and kinematic viscosity of each stream for the formulation of lecithin NPs

	Organic stream 1	Aqueous stream 2	Aqueous stream 3	Aqueous stream 4
$U_i$ (m/s)	0.12	0.36	0.36	0.36
$\nu_i$ (m <sup>2</sup> /s)	$0.54 \times 10^{-6}$	$0.89 \times 10^{-6}$	$0.89 \times 10^{-6}$	$0.89 \times 10^{-6}$

Table S4. Velocity and kinematic viscosity of each stream for the formulation of zein NPs

	Organic stream 1	EtOH/water stream 2	Aqueous stream 3	Aqueous stream 4
$U_i$ (m/s)	0.12	0.12	0.36	0.36
$\nu_i$ (m <sup>2</sup> /s)	$0.4 \times 10^{-6}$	$2.3 \times 10^{-6}$	$0.89 \times 10^{-6}$	$0.89 \times 10^{-6}$

### Lumefantrine calibration curves in the mobile phase of HPLC at 347 nm

The mobile phase of HPLC is ACN:water (60/40, v/v, both with 0.05 vol% trifluoroacetic acid)

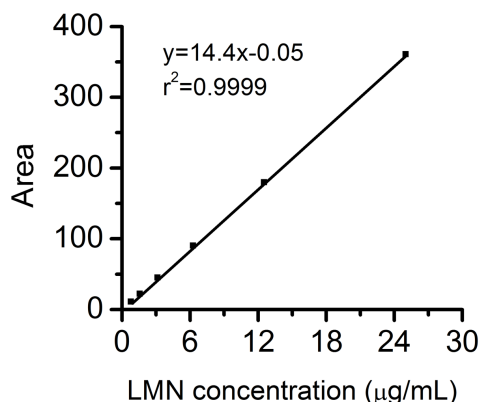


Figure S1. Calibration curve for lumefantrine dissolved in the mobile phase of HPLC at 347 nm

### NMR data for HPMCAS NPs

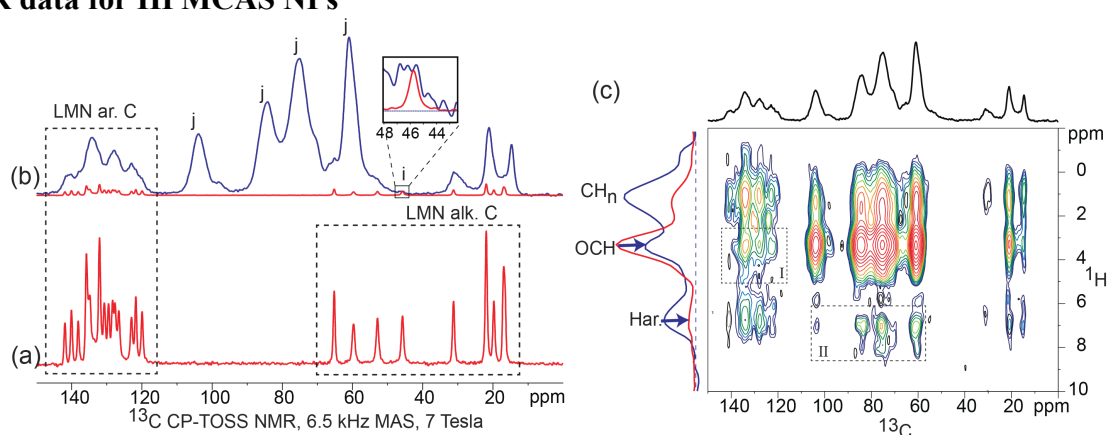


Figure S2.  $^{13}\text{C}$  CP-MAS solid-state NMR with total suppression of spinning sidebands (TOSS) of (a) bulk LMN (spectrum in red) and (b) HPMCAS NPs (spectrum in blue). The aromatic carbon (ar. C) and alkyl carbon (alk. C) signals of LMN are highlighted by dashed boxes. Peaks labelled “j” in (b) are the signals from the HPMCAS with minimal overlap from the LMN signal. Overlaid on (b) is the bulk LMN spectrum, scaled down to match the signal intensity of the residual crystalline LMN signal in the HPMCAS NPs. Inset in (b) shows the zoomed in fit of the residual crystalline LMN peak labelled “i”. (c) 2D  $^{13}\text{C}$ - $^1\text{H}$  HETCOR NMR of HPMCAS NPs acquired with 300 ms of  $^1\text{H}$  spin diffusion. The 1D  $^{13}\text{C}$  of the HPMCAS NPs is plotted along the top for reference.  $^1\text{H}$  spectra are plotted on the left, with the spectrum in blue and red corresponding to the  $^1\text{H}$  signal associated with the LMN and HPMCAS respectively. The dashed box labelled “I” represents the correlation signal between the aromatic carbons of the LMN the OCH protons of the HPMCAS. Conversely box labelled “II” represents the correlation signal between the OCH carbons of the HPMCAS and the aromatic protons of the LMN.

**References:**

1. Liu, Y., et al., *Mixing in a multi-inlet vortex mixer (MIVM) for flash nano-precipitation*. Chemical Engineering Science, 2008. **63**(11): p. 2829-2842.